[Frontiers in Bioscience 10, 905-918, January 1, 2005]

USE OF Mg^{2+} AND Ca^{2+} MACROELECTRODES TO MEASURE BINDING IN EXTRACELLULAR-LIKE PHYSIOLOGICAL SOLUTIONS

Dorothee Günzel [1], John A. S. McGuigan and Wolf-Rüdiger Schlue

Institut für Neurobiologie, Heinrich-Heine-Universität Düsseldorf, Universitätsstr. 1, 40225 Düsseldorf, Germany, [1] Present address: Institut für klinische Physiologie, Charité - Universitätsmedizin Berlin, Campus Benjamin Franklin, Hindenburgdamm 30, 12203 Berlin, Germany

TABLE OF CONTENTS

1. ABSTRACT

Macroelectrodes designed to measure the extracellular free Mg^{2+} and Ca^{2+} concentrations ($[Mg^{2+}]_o$, $[Ca^{2+}]_o$) may be used to determine Mg^{2+} and Ca^{2+} binding to extracellular buffers. This is important, as buffer concentrations may change physiologically or experimentally. A simplified calibration method allowed $[Mg^{2+}]_o$ and $[Ca^{2+}]_o$ > 50 µmol/l to be accurately measured. The method was used to determine the apparent

dissociation constant, K_{app} (± SD) of Mg^{2+} binding to aspartate (22°C, 101.7 ± 22.5 mmol/l, n = 8; 44°C, 45.2 ± 8.3 mmol/l, n = 6), citrate (high affinity, 0.33 ± 0.14 mmol/l, n = 4; low affinity, approximately 80 mmol/l), malate (15.9 ± 1.0 mmol/l, n = 7) and Ca^{2+} binding to malate (10.3 ± 1.1 mmol/l, n = 7). Calculated and measured K_{app} for Ca^{2+} binding to malate were only in agreement if the concept of ionic equivalent was used to adapt the tabulated constants to the experimental conditions. For Mg^{2+} binding to aspartate, malate and citrate there was no or only limited agreement with the calculated K_{app}. These findings emphasise the difficulties involved in calculating free concentrations in biological solutions. It is concluded that it is more accurate to measure K_{app} at the appropriate ionic strength and temperature.

2. INTRODUCTION

Magnesium research has been hampered by the difficulties in estimating both intracellular and extracellular free magnesium concentrations. These difficulties arise mainly from a lack of sensors with sufficient selectivity for Mg^{2+}, over Ca^{2+}, H^+, Na^+ and K^+. However, over the past 15 years, Mg^{2+}-selective microelectrodes and fluorescence dyes have been greatly improved and successfully applied to measure intracellular free magnesium concentrations ($[Mg^{2+}]_i$) and its regulation in a variety of tissues. These intracellular techniques have been recently reviewed in detail (8, 24). The present work therefore concentrates on the measurement of the extracellular free Mg^{2+} concentration ($[Mg^{2+}]_o$).

Over the past decade, commercially available analysers had been developed for the routine determination of $[Mg^{2+}]_o$ in plasma or serum. The major source of error in the determination of $[Mg^{2+}]_o$ is the presence of mmol/l extracellular Ca^{2+} concentrations which reduces the selectivity of the electrode. To measure $[Mg^{2+}]_o$, a simultaneous estimation of $[Ca^{2+}]_o$ is essential to correct for the Ca^{2+} interference. In a direct comparison of three of these analysers, the lack of selectivity of the electrode and the correction necessary for $[Ca^{2+}]_o$ resulted in discrepancies amongst the measured $[Mg^{2+}]_o$ for identical samples (15).

The total Mg^{2+} concentration in human serum lies between 0.7 and 1.1 mmol/l (30) with the free form accounting for 60 to 80% of the total (28). The Mg^{2+} is mostly bound to protein (some 85% of the bound Mg^{2+}) and the remaining 15% complexed to bicarbonate or organic anions (14). The total combined concentrations of malate, citrate, pyruvate and lactate in human plasma amount to about 1 mmol/l (table 1 in Ref 24). In contrast, in invertebrates, the amount of extracellularly bound Mg may be considerably larger. The blood of the medicinal leech, *Hirudo medicinalis*, contains up to 30 mmol/l malate and considerable amounts of other organic ions such as α-ketoglutarate or succinate (13). As estimated from published dissociation constants (19, 20), malate alone may account for a binding of some 75% of the total extracellular Mg^{2+} in this organism.

The Mg^{2+}-sensors ETH 7025 and ETH 5506 have been used to manufacture macroelectrodes capable of measuring $[Mg^{2+}]_o$ at µmolar concentrations in intracellular and extracellular-like physiological solutions respectively (17, 23). Macroelectrodes with ETH 7025 have also been used to measure the apparent binding constant of Mg^{2+} to ATP in an intracellular-like background solution (18, 35). More recently, macroelectrodes manufactured with ETH 5506 were used to measure Mg^{2+} efflux in 1 ml of atrial cell suspensions in the presence of 0.9 mmol/l $[Ca^{2+}]_o$ (see figure 2 in Ref. 24). The most recent sensor ETH 5504 (36), which shows even greater selectivity over Ca^{2+} than ETH 5506, has been used in microelectrodes (8) but has not yet been used to manufacture macroelectrodes for application in extracellular-like physiological solutions. Similar electrodes are also available to measure other ions, *e.g.* Ca^{2+}-selective macroelectrodes based on the sensor ETH 1001 (6).

These experimental procedures required not only calibration solutions in the range from 0.25 mmol/l to 10 mmol/l but also the appropriate Ca^{2+} and Mg^{2+} buffer solutions for the concentration range ≤ 0.1 mmol/l. However, the manufacture of accurate buffer solutions is not only tedious but also time consuming, limiting the application of this method (17, 21). In the present paper a method will be described to accurately measure Mg^{2+} and Ca^{2+} concentrations greater than 50 µmol/l. In this approach the macroelectrodes are calibrated in the range from 0.25 mmol/l to 10 mmol/l, a range in which buffer solutions are unnecessary. This is coupled with one single calibration solution in which $[Mg^{2+}]_o$ and $[Ca^{2+}]_o$ have been reduced to less than $10^{-7.5}$ mol/l (pX, 7.5) by the addition of the appropriate chelator to a nominally Mg^{2+}- or Ca^{2+}-free calibration solution.

The binding of Mg^{2+} to aspartate, malate and citrate was studied using this approach. Aspartate was chosen because of the clinical use of this anion (4) and because the binding of Mg^{2+} to aspartate, with the concomitant reduction of the $[Mg^{2+}]_o$ has been postulated to be the reason why intravenous application of Mg-di-asparate in animal experiments failed to reduce the infarct size in the heart, whereas administration of $MgSO_4$ did (7).

The binding of Mg^{2+} to malate and citrate and Ca^{2+} to malate were measured because of the importance of these anions in studies on Mg^{2+} regulation in leech neurones; malate being the major extracellular anion in this organism, even surpassing the extracellular Cl^- concentration (13). Furthermore, malate and citrate appear to be directly involved in the regulation of $[Mg^{2+}]_i$ in the neurones of this organism, possibly through a Na^+-independent cotransport system for Mg^{2+} and organic anions (9). Thus, malate may not only be responsible for the extracellular Mg^{2+} binding, but also be an important factor for the intracellular Mg^{2+} buffering. Citrate could also play a role in the extracellular buffering of Mg^{2+} and Ca^{2+} in the nervous system. Astrocytes actively transport citrate into the extracellular fluid (33). Since citrate chelates both Mg^{2+} and Ca^{2+}, the citrate concentration regulates both the $[Mg^{2+}]_o$ and $[Ca^{2+}]_o$ and Westergaard *et al*. (33) have postulated that the citrate concentration indirectly modulates the neuron excitability.

The results illustrate that Mg^{2+} macroelectrodes based on the sensors ETH 5506 and Ca^{2+} macroelectrodes manufactured with ETH 1001 can be a valuable tool for the investigation of Mg^{2+} or Ca^{2+} binding. There is need for such an approach as the free concentrations calculated from published dissociation constants generally differ from the measured free concentrations (see Discussion).

3. MATERIALS AND METHODS

3.1. Macroelectrodes

Macroelectrodes were manufactured as previously described (17). The Mg^{2+} macroelectrodes were based on the Mg^{2+} sensor ETH 5506 (26) while the Ca^{2+} macroelectrodes were based on the Ca^{2+} sensor ETH 1001 (27). The macroelectrodes were backfilled with 150 mmol/l $MgCl_2$ or $CaCl_2$. A macroelectrode filled with 3 mol/l KCl was used as a reference electrode.

3.2. Experimental set-up/Recording

A diagram of the experimental set-up has been described in Zhang *et al.* (34) and only a brief summary is given here. 100 ml of the appropriate solution was titrated with either $MgCl_2$ or $CaCl_2$, and continuously stirred using a magnetic stirrer. To prevent heating of the solution the beaker was insulated from the magnetic stirrer with cork matting. A custom built electrode holder allowed the electrodes to be rapidly removed or replaced in the solution. Potential recording was with a WPI high-impedance amplifier and an Orion pH/mV meter. The output signals were AD converted and recorded by computer allowing the time course of the changes to be observed. A Faraday cage was used to reduce electrical interference to a minimum.

3.3. Solutions

3.3.1. Background solutions

Solution 1 was a high K^+ solution and contained in mmol/l: K^+, 140; Cl^-, 124; Hepes, 5, pH 7.4. Solution 2 was a high Na^+ solution: Na^+, 90; K^+ 4; Cl^-, 89; Hepes 10, pH 7.4. When present, the aspartate concentration as aspartic acid was 10 mmol/l, the citrate concentration as Na_3Citrate was 10 mmol/l and the malate concentration as Na_2Malate was either 10 mmol/l (Mg^{2+} measurements) or 30 mmol/l (Ca^{2+} measurements). In all cases, the total Na^+ concentration in Solution 2 was maintained at 90 mmol/l by appropriate omission of NaCl. Solution 3 was used to measure the binding of Mg^{2+} to aspartate at a temperature corresponding to the body temperature of the dog (39°C) and contained in mmol/l: Na^+, 140; Cl^-, 135; Hepes, 10. pH is temperature dependent and for an exact measurement of pH both calibration of the pH electrode and measurement of pH have to be carried out at the same temperature (19). To simplify the pH calibration procedure in this case, the pH was adjusted to 7.68 at 22°C, which corresponds to a pH of 7.4 at 40°C (3). Aspartate concentration as aspartic acid was 10 mmol/l with maintenance of total Na^+ at 140 mmol/l.

3.3.2. Calibration solutions

Calibration solutions were identical to the respective background solutions. They were manufactured by adding the appropriate volume of $MgCl_2$ or $CaCl_2$ from a 1 mol/l or a 0.1 mol/l stock solution (Fluka, Germany) to 100 ml of background solution to give nominal concentrations of 10, 6, 4, 1.5 0.8, 0.5 and 0.25 mmol/l. These nominal concentrations were corrected for the slight dilution effect caused by the increase in volume to give actual concentrations of 9.901, 5.964, 3.984, 1.477, 0.793, 0.497 and 0.249 mmol/l respectively. To obtain a solution with a pMg/pCa greater than 7.5, 0.2 mmol/l EDTA or EGTA was added to the respective Mg^{2+} and Ca^{2+} free background solution.

3.3.3. Pipettes

The same pipette was used for titration experiments and measurement of the calibration solutions. In the initial experiments an Eppendorf pipette was used. Later a Socorex 411 Stepper pipette was employed (accuracy ± 1%). A 100 ml pipette (Brand, accuracy ± 0.08%) was used for volume measurement in the titration experiments. The pipettes were calibrated by weighing.

3.4. Temperature

With the exception of Mg^{2+} binding to aspartate in solution 3, all experiments were carried out at room temperature, 22°C. To measure Mg^{2+} binding to aspartate at a temperature similar to the body temperature of the dog (39°C), the background and aspartate solution were heated to 44°C in an oven. Titration was carried out in a 100 ml beaker which had been isolated with Bubble Wrap® and the measurements were carried our rapidly.

3.5. Macroelectrode calibration

Macroelectrodes were calibrated using the Mg^{2+} or Ca^{2+} calibrating solutions (17, 21). Calibration has normally been carried out by commencing measurement in the nominal 10 mmol/l calibration solution, waiting until a steady state has been reached (3 minutes or more), removing the macroelectrode, washing with distilled water, wiping the drops off with Kleenex® tissue and dipping into the next calibration solution (17). The method has the disadvantage of large voltage swings on solution change. In this series of experiments the method was modified in that on changing from one calibration solution to the next, the macroelectrode was quickly dipped into around 50 ml of the next calibration solution. After a few seconds wash in this solution, the electrode was quickly removed and placed in the actual calibration solution. This method considerably reduced the potential swings on solution change. The calibration solutions were kept covered with Parafilm® to prevent evaporation and a slow increase in the concentration. Evaporation loss cannot be neglected. In a 100 ml beaker filled with 60 ml of solution 0.14 ml is lost per hour as measured by weight loss over 30 hours. Over the course of 24 hours this would cause an increase of around 0.6 mmol/l; equivalent to a change of some 0.6 mV.

Calibration was started in the nominal 10 mmol/l solution and then downwards to the 0.25 mmol/l calibration solution. The solution was then changed to the nominally Mg^{2+}/Ca^{2+} free background solution and finally to the background solution with either EGTA or EDTA, before returning to the 10 mmol/l calibration solution to estimate the drift. In the calibration solutions three minutes were sufficient to reach a steady state; in the nominally Mg^{2+}/Ca^{2+}

free background solutions and in the EGTA/EDTA solutions the time was increased to five minutes.

The potential in the 10 mmol/l calibration solution was defined as relative zero and all potentials were referred to this zero potential. Drift was measured in one experiment and found to be linear over a six hour period. Potentials were corrected to the arbitrary zero on the basis of a linear drift.

3.6. Titration experiments

3.6.1. Titration of background solution

Since no Mg^{2+} or Ca^{2+} buffer solutions were used in these experiments, it was possible to validate the calibration of the macroelectrodes by titrating the background solution from 0.25 mmol/l upwards to 10 mmol/l. This approach has the advantage that a direct comparison between the free concentrations in the background solution and in the background solutions plus the organic anions was possible.

The procedure commenced with potential measurement in the 10 mmol/l calibrating solution. When a steady state was reached in this solution the calibrating solutions were changed to 4 mmol/l, 0.8 mmol/l, 0.25 mmol/l, nominally Mg^{2+}/Ca^{2+} free background solution and then the EDTA or EGTA solutions. At this point the titration was started with 100 ml of the background solution containing 0.25 mmol/l Mg^{2+} or Ca^{2+}. Titration was from 0.25 mmol/l, 0.5 mmol/l, 1 mmol/l and then in steps of 1 mmol/l until 10 mmol/l. At the end of the titration the potential in the 10 mmol/l calibration solution was again measured in order to estimate any drift in the electrode. The dilution effect of the titration was taken into account.

3.6.2. Titration of background solution containing organic anions

After the control titration of the background solution without organic anions up to four titrations of the background solution with organic anion were carried out, after which background titration was again performed. The average of the two background titration curves were used as calibration to calculate the free concentrations in the organic anion solutions.

4. RESULTS

4.1. Macroelectrodes

4.1.1. Drift

To make accurate measurements, drift of the electrodes must be as low as possible. Drift was minimized though not entirely eliminated by preventing warming of the solution due to the heat produced by the magnetic stirrer by insulating the beaker with cork matting and by using adequately chlorided silver wires. In 5 of the Mg^{2+} experiments the maximum changes were ± 2 mV/hour. In the other two experiments the maximum changes were greater, being 3.75 and 2.8 mV per hour respectively. The results with the three Ca^{2+} experiments were similar to the five Mg^{2+} experiments.

The apparent change in concentration ($\Delta[X^{2+}]$) due to drift (± ΔE) is a function of the slope of the macroelectrode and the initial concentration ($[X^{2+}]_1$). It can be calculated as follows:

$$\Delta[X^{2+}] = [X^{2+}]_1 (10^{\frac{\pm \Delta E}{s}} - 1) \qquad [1]$$

The mean slope of the Mg^{2+} and Ca^{2+} macroelectrodes was 23.516 and 27.387 mV/decade respectively. For Mg^{2+}, a ± 2 mV/hour drift corresponds, at an initial concentration of 10 mmol/l to an apparent increase of 2.16 mmol/l for a positive drift and to an apparent decrease of 1.78 mmol/l for a negative drift. The corresponding apparent changes for Ca^{2+} are an increase of 1.83 mmol/l and a decrease of 1.54 mmol/l. At 0.25 mmol/l the apparent changes would be an increase of 0.05 mmol/l or a decrease of 0.04 mmol/l for Mg^{2+} and for Ca^{2+} an increase/decrease of 0.04 mmol/l.

4.1.2. Comparison between the two methods of calibration

Since calibration using calibration solutions was from 10 mmol/l downward and titrating the background solution was from 0.25 mmol/l up to 10 mmol/l, a check was initially made to see if both methods gave the same result i.e. the macroelectrodes did not exhibit hysteresis. Figure 1A shows the results of two measurements using calibration solutions and two measurements in which the background solution was titrated. The results from both methods are very similar, which means the electrodes showed no hysteresis. To check the accuracy of the background titration experiments, the two measurements in the calibration solutions were combined and fitted by the Nicolsky-Eisenman equation. This equation was then used to calculate the potentials from 0.1 mmol/l to 10 mmol/l. The combined titration measurements were also fitted with the Nicolsky-Eisenman equation and the equations used to estimate the concentrations from the calculated potentials (22). The differences were minimal; at 0.1 mmol/l it was 1.2 % and declined towards zero as the concentration increased. Similar results were obtained in a second experiment.

4.1.3. Reproducibility

To check reproducibility three background solutions were titrated. The first and third titrations were used to calibrate the electrode and the $[Mg^{2+}]$ concentrations were estimated from the potential measurements in the second titration. The results of such an experiment are illustrated in figure 1B. The regression line drawn through the estimated $[Mg^{2+}]$ had a slope of 0.9897 indicating good reproducibility.

4.1.4. Extension of calibration to lower concentration values

Mg^{2+} and Ca^{2+} contamination of unbuffered solutions has been reported to be in the order of 20 µmol/l. Calibration solutions below 0.25 mmol/l cannot therefore be manufactured by simple dilution. While buffered Mg^{2+} or Ca^{2+} solutions (17, 21) could be used to extend calibrations to lower concentrations, such an approach is intricate and often not feasible. Therefore, a simpler although less exact method was chosen whereby the potential was measured in solutions to which 0.2 mmol/l of

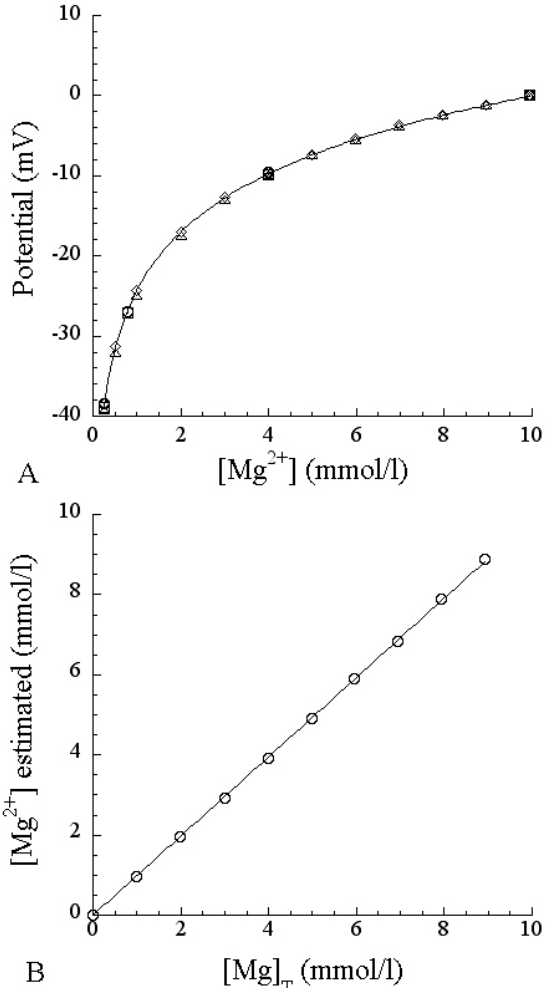

Figure 1. A. Comparison between the two methods of calibration. Open circles and squares: calibration carried out using standard solutions. Open triangles and diamond: calibration by titrating the background solution. The fit to the combined curves in both solution calibration and the titration method with the Nernst equation was:

Calibration solutions:

$$Potential = 48.6476 + 24.3327 \cdot \log\left(\frac{[Mg^{2+}]}{1000}\right);\ r = 0.999845$$

Background Titration:

$$Potential = 48.8107 + 24.4034 \cdot \log\left(\frac{[Mg^{2+}]}{1000}\right);\ r = 0.999836$$

B. Blank background titration. The linear regression drawn through the points was: $[Mg^{2+}] = 0.9897*[Mg]_T$; r = 0.999978.

EGTA or EDTA had been added. This is some ten times greater than the expected maximum contamination of 20 µmol/l (21); since the actual contamination level was initially unknown, the pX values in the EDTA/EGTA solutions was assumed to be at least 7.5 for both Mg^{2+} and Ca^{2+} (see Discussion). With these assumptions, typical calibration curves for both Mg^{2+} and Ca^{2+} macroelectrodes are illustrated in figure 2. The curves show that the Ca^{2+} macroelectrodes are more selective than the Mg^{2+} macroelectrodes. As will be shown in the Discussion, this method of calibration, while not exact, does allow determination of concentrations greater than 50 µmol/l for both Mg^{2+} and Ca^{2}.

4.2. Magnesium binding studies

4.2.1. Aspartate

Four experiments with aspartate present were carried out in a high K^+ background (solution 1) and four in a high Na^+ background (solution 2). The presence of Na^+ *versus* K^+ did not alter the results; therefore, the experiments were pooled. A typical plot of the free $[Mg^{2+}]$ against bound Mg^{2+} is illustrated in figure 3A. There is a small but significant binding of Mg^{2+} to aspartate. Because the binding of magnesium to aspartate was small it was not possible to distinguish if Mg^{2+} bound one or two aspartate molecules. To fit the curves the simplest assumption was made, namely, that aspartate binds one Mg^{2+}. Under these conditions (35):

$$\left[X - Anion^{(n-2)-}\right] = \frac{\left[X^{2+}\right][Anion]_T}{\left(K_{app} + \left[X^{2+}\right]\right)} \qquad [2]$$

where $[X\text{-}Anion^{(n-2)-}]$ is the bound concentration, $[Anion]_T$ the total anion concentration, $[X^{2+}]$ the free concentration and K_{app} the apparent dissociation constant for either Mg^{2+} and Ca^{2+}. A typical fit to equation [2] for aspartate is shown in figure 3A. In the fit, the aspartate concentration was taken to be 10 mmol/l. The K_{app} in this experiment was 97.2 mmol/l. The mean ± SD for the K_{app} from eight experiments was 101.7 ± 24.0 mmol/l. Another way of presenting the data is illustrated in figure 3B. In this Figure, the results from all eight experiments have been plotted as the $[Mg]_T$ (*x* axis) against the $[Mg^{2+}]$ (*y* axis). The dashed line represents the case in which there would be no binding of Mg^{2+} to aspartate. Since the measured $[Mg^{2+}]$ lies below this line, a small fraction of Mg^{2+} must be bound to aspartate.

To calculate the free $[Mg^{2+}]$ at a given $[Mg]_T$ the following quadratic equation must be solved::

$$\left[X^{2+}\right] = \frac{-\left([Anion]_T + K_{app} - [X]_T\right) + \sqrt{\left([Anion]_T + K_{app} - [X]_T\right)^2 + 4K_{app}[X]_T}}{2} \qquad [3]$$

To fit data from individual experiments, K_{app} in equation [3] was varied until the best fit, as judged by eye, was obtained. Although not a curve fitting routine, it gave very similar results, mean ± SD being 101.0 ± 22.5 mmol/l, supporting the curve fitting routine used in figure 3A. The mean value for K_{app} of 101.7 mmol/l was used to fit the combined results, and this is shown as the continuous line in figure 3B.

To mimic Mg^{2+} binding to aspartate in the experiments of Grunert *et al.* (7) experiments were carried out in solution 3 at temperatures of about 40 °C. In this temperature range, the mean ± SD for K_{app} was reduced from 101.7 ± 24.0 mmol/l at 22°C to 45.2 ± 8.3 mmol/l (n = 6). This estimation is only an approximation as the temperature control was not exact (see Discussion).

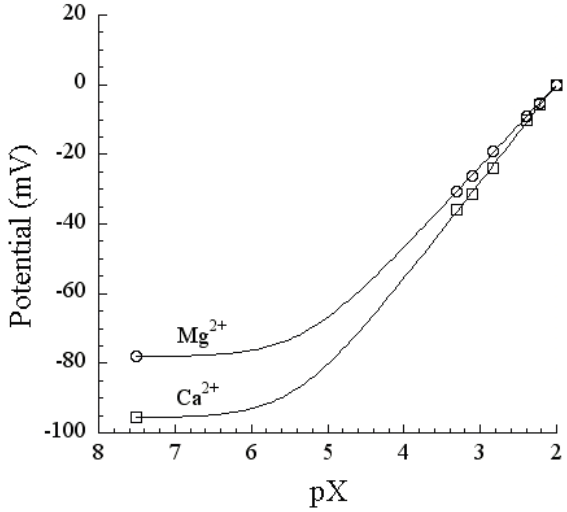

Figure 2. Typical calibration curves for Mg^{2+} (upper curve) and Ca^{2+} (lower curve). The fits by the Nicolsky-Eisenman equation to the curves were: Mg^{2+}: Potential = 47.1612 + 23.5806*log(10^{-pMg} + 4.81*10^{-6}); r = 0.999972. Ca^{2+}: Potential = 56.2552 + 28.1276*log(10^{-pCa} + 3.91*10^{-6}); r = 0.999838. For comparison, the mean ± SD for all electrodes was: Mg^{2+}: Potential = 47.0323 ± 3.8738 + 23.5161 ± 1.9369*log(10^{-pMg} + 2.95 ± 1.85*10^{-6}); n = 11. Ca^{2+}: Potential = 54.7756 ± 1.2393 + 27.3878 ± 0.6195*log(10^{-pCa} + 3.06 ± 0.48*10^{-6}); n = 7.

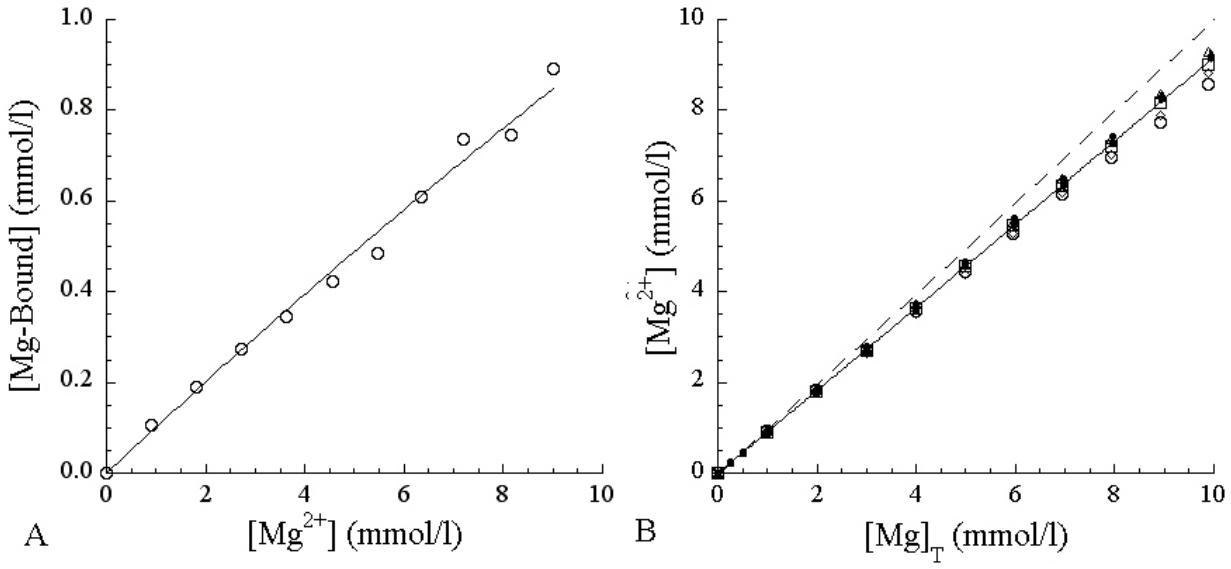

Figure 3. Aspartate. A. Plot of $[Mg^{2+}]$ against [Mg-Bound]. The points have been fitted using equation [2], with an $[Aspartate]_T$ of 10 mmol/l. In this fit K_{app} was 97.2 mmol/l and r = 0.994819. B. Combined plot of $[Mg]_T$ against $[Mg^{2+}]$ (n = 8). The interrupted line represents equality between $[Mg]_T$ and $[Mg^{2+}]$, *i.e.,* no binding. The solid line drawn through the points was calculated using the mean K_{app} of 101.7 mmol/l and equation.

4.2.2. Malate

Nine experiments were performed, five in solution 1 and four in solution 2. From the five experiments in solution 1, two were more than one SD from the mean K_{app}. The reason for this is unclear but because of the wide deviation from the mean value they have been excluded from the pooled results of the other seven experiments. The results are presented in figure 4 in a similar manner to that of figure 3. The mean value ± SD for the K_{app} for malate estimated from free/bound plots was 15.8 ± 1.0 mmol/l; the mean ± SD calculated from total/free plots was again very similar, namely 15.5 ± 1.0 mmol/l.

4.2.3. Citrate

Four experiments were performed with citrate in a high Na^+ background solution, solution 2. In two experiments the $[Mg]_T$ was 10 mmol/l and in two, 20 mmol/l. In the experiments with 20 mmol/l $[Mg]_T$, the bound Mg was slightly greater than the total citrate concentration of 10 mmol/l, suggesting the formation of a

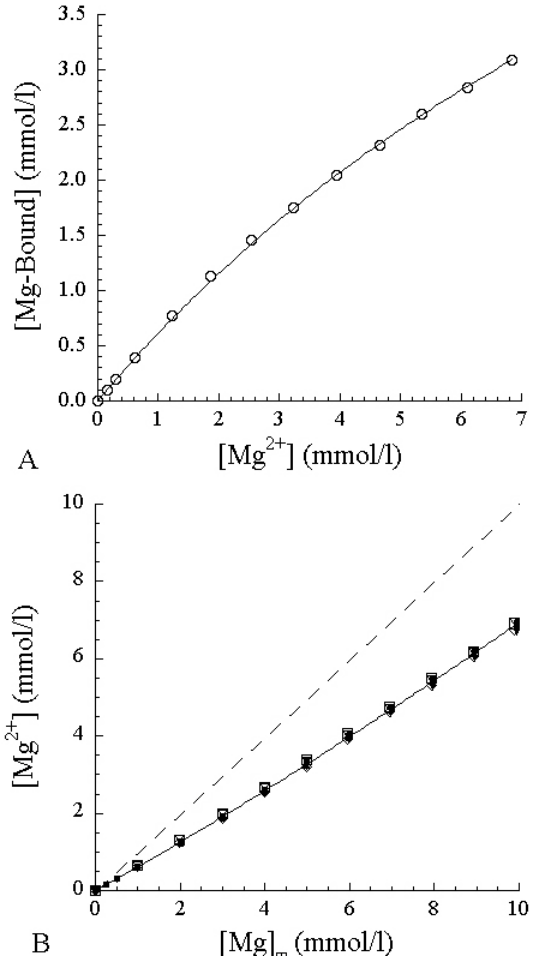

Figure 4. Malate. **A** and **B** similar to Figure 3. For the curve fit to **A**, $[Malate]_T$ was 10 mmol/l, K_{app} was 15.3 mmol/l and r = 0.999834. The solid line in **B** was calculated as in Figure 3B using the mean K_{app} of 15.8 mmol/l (n = 7).

di-Mg citrate complex. Under these circumstances the bound Mg is given by:

$$[X-Anion]_B = \frac{\left[X^{2+}\right][Anion]_T}{\left(K_{app}+\left[X^{2+}\right]+\frac{\left[X^{2+}\right]^2}{K_2}\right)} + \frac{2\left[X^{2+}\right]^2[Anion]_T}{K_2\left(K_{app}+\left[X^{2+}\right]+\frac{\left[X^{2+}\right]^2}{K_2}\right)} \quad [4]$$

where K_{app} and K_2 are defined as follows:

$$K_{app} = \frac{\left[X^{2+}\right]\left[Anion^{n-}\right]}{\left[X-Anion^{(n-2)-}\right]} \quad [5]$$

$$K_2 = \frac{\left[X^{2+}\right]\left[X-Anion^{(n-2)}\right]}{\left[X_2-Anion^{(n-4)-}\right]} \quad [6]$$

The result of fitting equation [4] to the data is illustrated in figure 5A. In this experiment K_{app} was 0.31 mmol/l and the mean ± SD for the four experiments was 0.33 ± 0.14 mmol/l. The estimation of K_2 cannot be regarded as accurate because only two experiments were carried out, and as both $[Mg]_T$ and free $[Mg^{2+}]$ are increased towards 20 mmol/l and 10 mmol/l respectively, the accuracy of the measurements declines. In the experiment in figure 5A, K_2 was 57.2 mmol/l and in the second experiment it was 182 mmol/l.

In the two-binding-site model, $[Mg^{2+}]$ can be calculated from the following cubic equation:

$$\left[Mg^{2+}\right]^3 + \left(K_2 + 2[Anion]_T - \left[Mg^{2+}\right]_T\right)\left[Mg^{2+}\right]^2 + \\ + \left(K_{app}K_2 + [Anion]_T K_2 - \left[Mg^{2+}\right]_T K_2\right)\left[Mg^{2+}\right] - \left[Mg^{2+}\right]_T K_{app}K_2 = 0 \quad [7]$$

The pooled results for $[Mg]_T$ and free $[Mg^{2+}]$ are shown in figure 5B. The results have been fitted using the mean K_{app} value of 0.33 mmol/l and a value for K_2 of 80 mmol/l. This latter value, while between the two determined values, is rather arbitrary, and was chosen to give the best fit as judged by eye. As shown in figure 5B a two-site model gave a better fit to the data than simply assuming one to one binding.

4.3. Calcium binding studies

4.3.1. Malate

Five experiments were carried out in solution 2 and two additional experiments in solution 2 with 2.4 mmol/l Mg^{2+}. No difference was seen as a result of adding Mg^{2+}, so all 7 results have been pooled. The results are presented in figure 6A and B. The mean ± SD for K_{app} was 10.3 ± 1.1 mmol/l from an ionised/bound plot. The same result was obtained from a total/ionised plot.

5. DISCUSSION

5.1. Accuracy of the method

5.1.1. General accuracy

Despite the several precautions noted (see "Methods") there was drift of the macroelectrodes in the order of 2 mV per hour. The drift of the macroelectrode was systematically checked during the course of an experiment by measuring the potential in the 10 mmol/l calibration solution. Any changes in this potential were due to electrode drift and on the assumption that it was linear, the drift could be compensated for. These precautions made it possible to measure the small but significant binding of Mg^{2+} to aspartate as is shown in figure 3.

5.1.2. Extension of calibration to lower concentration values

This procedure is based on the potential measurement in a calibration solution containing either EDTA (Mg^{2+}) or EGTA (Ca^{2+}) and assuming that the pX is greater than 7.5. As illustrated in the calibration curves in figure 2, the lower ranges of the curve (pX > 5) are largely dependent on the measured potential in the chelator containing solutions and to some extent on the assumed pX value. The accuracy of the procedure was checked by using the Nicolsky-Eisenman equation to investigate 1) the extent of a variation in the potential measurement at these pX values and 2) the degree to which a change in the assumed pX value of the EDTA/EGTA solutions would affect the calculated concentrations.

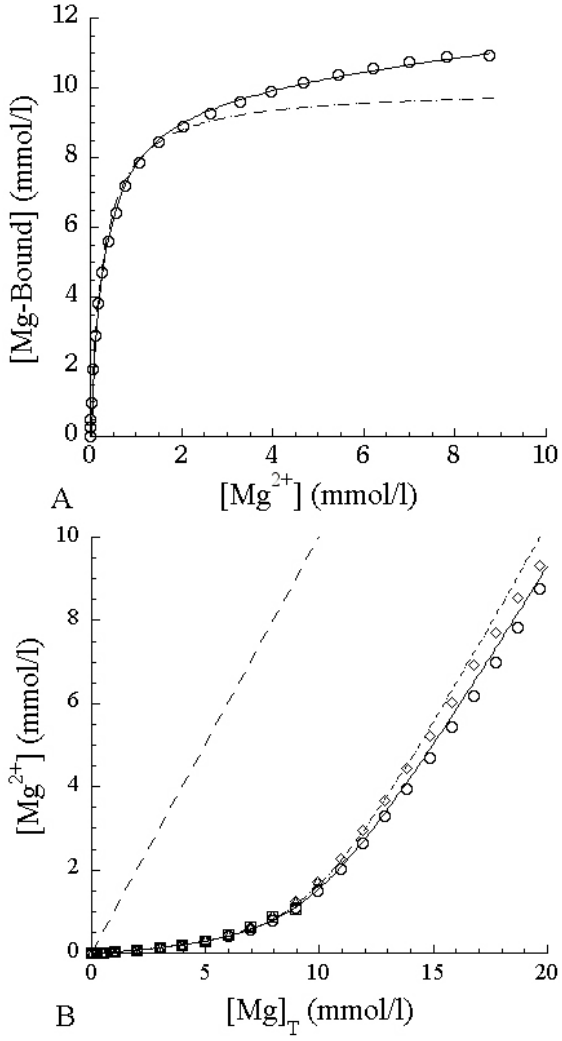

Figure 5. Citrate. **A.** Plot of $[Mg^{2+}]$ against [Mg-Bound], but the points have been fitted assuming two bindings sites with equation [4] and a $[Citrate]_T$ of 10 mmol/l. K_{app} was 0.31 mmol/l and K_2 57.17 mmol/l and r = 0.999840. The interrupted line is drawn on the assumption of only one binding site equal to K_{app}. **B.** Similar to Figure 3B, but the $[Mg^{2+}]$ was calculated from equation [7], using the Newton-Raphson method. The mean value of K_{app} of 0.33 mmol/l was used. The value of K_2 of 80 mmol/l was assumed. The interrupted line is drawn on the assumption of only one binding site. For further details see text (n = 4).

The Nicolsky-Eisenman characteristics from the 11 different calibration curves were averaged and the mean curve is illustrated as the continuous line in figure 7A. Over a week's experimentation with an electrode, the maximum change in the potential measured in the EDTA solution was 4.85 mV. Because of this, the influence of ± 5 mV variation from the mean curve at a pMg value of 7.5 was investigated. These variations were also fitted with the Nicolsky-Eisenman equation and the ± 5 mV deviations are illustrated as the dashed curves in figure 7A. The difference these deviations from the actual potential make to the calculated concentrations can be estimated by using the potentials calculated from the mean curve, to estimate the concentrations using the curves obtained when there was a deviation of the potential at pMg of 7.5. The ratio, true/estimated concentration in the range 1 µmol/l to 200 µmol/l for deviations of ± 5 mV is illustrated in figure 7B. At concentrations below 50 µmol/l the deviation from a ratio of one increases rapidly. As the concentrations increase above 50 µmol/l, the error becomes smaller. A similar result was obtained when pMg values were varied from 6 to 7.5 (calculations not shown). Calculations for calcium gave similar results. It can therefore be concluded that this method of extending the range of the macroelectrode below the range of normal calibration solutions is accurate at concentrations greater than 50 µmol/l. Below this range, buffer solutions would have to be used for accurate measurements.

5.2. Background contamination

Using both solution calibration and background titration methods, the contamination level for both Mg^{2+} and Ca^{2+} was estimated. The mean ± SD was 8.4 ± 5.9 µmol/l (n = 14) and 6.3 ± 0.75 µmol/l (n = 9) for Mg^{2+} and Ca^{2+}, respectively. However, these values lie in the range of concentrations where the methods cannot be regarded as accurate. A ± 5 mV deviation at pMg 7.5 would give a range for Mg^{2+} contamination from 5.1 µmol/l to 13.8 µmol/l from the mean value of 8.4 µmol/l and for Ca^{2+} from 4.7 µmol/l to 7.3 µmol/l. Changing from pX 7.5 to 6.5 and assuming the same difference between the potential in the chelator and background solutions did not significantly alter the estimated mean background contamination concentrations. It thus seems fair to conclude that the contamination levels in each case were on the order of 10 µmol/l. An accurate determination of the contamination using macroelectrodes would require buffer solutions.

An upper limit can be set to the Mg^{2+} and Ca^{2+} free concentrations by measuring the total concentration by atomic absorption spectrometry. If there is no binding or only limited binding of either Mg^{2+} or Ca^{2+} as would be the case in solutions without chelators, then the total concentration would approximate the free concentration. Such a determination was carried out for Mg^{2+} and a value of 5 µmol/l was found. If the Ca^{2+} contamination was similar and since the Mg^{2+} macroelectrode at these concentrations reacts to both Mg^{2+} and Ca^{2+}, this would give a combined contamination of 10 µmol/l, in the range of the estimated value. Thus the measured value of the inherent contamination of solutions is 5 to 10-fold lower than the 50 µmol/l resolution of the macroelectrode method.

5.3. Binding of Mg^{2+} and Ca^{2+} to organic anions

Two aspects will be considered, namely 1) how closely do calculated and measured K_{app} agree with each other and 2) under what conditions might the binding of either Mg^{2+} or Ca^{2+} to the organic anions have physiological significance.

5.3.1. Comparison between calculated and measured K_{app} values

The calculation of the K_{app} values for the binding of Mg^{2+} to aspartate, malate and citrate and the binding of

Table 1. Calculation of the single-ion H^+ activity coefficient to convert pH_a to pH_c

Solutions	Ionic strength	Ionic-equivalent	Single ion activity coefficient				pH_c		ΔpH_c
	(mol/l)	(mol/l)	Davies	H & W	H & B	Bates	Davies	H & W	
Magnesium									
Constants	0.1000	0.1000	0.7724	0.7978	0.7839	0.7776	7.2878	7.3019	0.0141
Aspartate-Na^+	0.1140	0.1090	0.7639	0.7917	0.7776	0.7689	7.2831	7.2986	0.0155
Malate-Na^+	0.1040	0.0940	0.7698	0.7959	0.7821	0.7751	7.2864	7.3009	0.0145
Citrate-Na^+	0.0990	0.0890	0.7731	0.79834	0.7844	0.7783	7.2882	7.3022	0.0140
Aspartate-K^+	0.1532	0.1432	0.7453	0.7788	0.7626	0.7488	7.2724	7.2914	0.0191
Malate-K^+	0.1532	0.1432	0.7453	0.7788	0.7626	0.7488	7.2724	7.2914	0.0191
Calcium									
Malate-Na^+	0.124	0..0940	0.7586	0.7878	0.7734	0.7632	7.2800	7.2965	0.0164

Abbreviations: Davies: Davies (1967); H & W: Hamer & Wu (1972); H & B: Harrison & Bers (1989); Bates: Bates (1973).

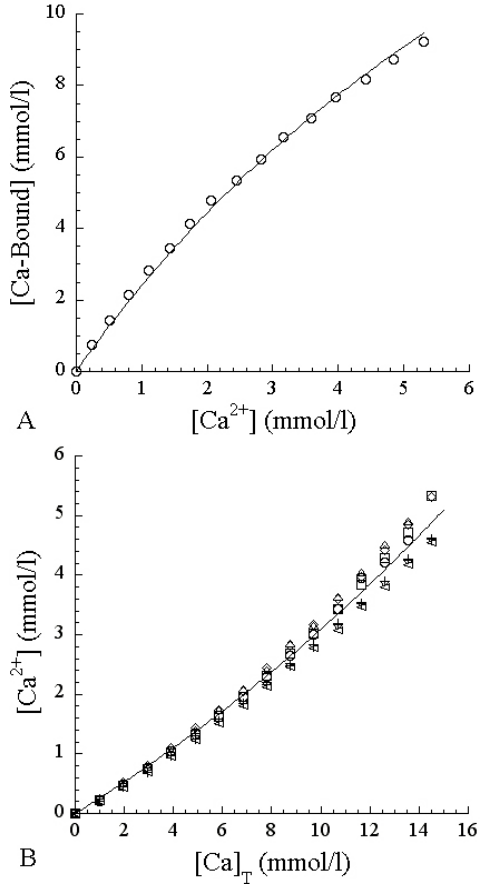

Figure 6. Malate. **A.** Plot of $[Ca^{2+}]$ against [Ca-Bound]. Equation [2] and a $[Malate]_T$ of 30 mmol/l; K_{app} was 11.5 mmol/l and r = 0.998602. **B.** Combined results of the experiments plotted as in Figure 3B (n = 7). The mean K_{app} of 10.3 mmol/l was used to draw the line through the points.

Ca^{2+} to malate from the tabulated constants in Martell & Smith (19, 20) involves three steps 1) conversion of pH_a to pH_c, 2) correction of the tabulated constants to the appropriate ionic strength and 3) temperature corrections for 1 and 2. In the following calculations no temperature correction has been made since the experiments were carried out at room temperature and the tabulated constants are normally for 20°C or 25°C. To convert from the measured H^+-ion activity to H^+-ion concentration it is necessary to estimate the single-ion activity coefficient of H^+ ions (γ_+); there are four methods of doing this. In the first three, the assumption is made that mean activity coefficient for ions is equal to the single-ion activity coefficient (22). The mean activity coefficient can be calculated according to Davies (5), Hamer & Wu (10) and Harrison & Bers (11) or the single-ion activity coefficient can be calculated directly according to Bates (2). The four methods gave different results and γ_+ for H^+ calculated for the ionic strengths of the solutions used in these experiments are summarised in table 1. The single ion activity coefficient varied according to the method chosen. The maximum values were those calculated from Hamer & Wu (10) and the minimum values using the equation from Davies (5). These two extreme values for γ_+ for H^+ were used to calculate the pH_c values for a pH_a of 7.4, and the maximum and minimum pH_c values are also given in table 1.

The ionic strength, I is defined as follows (1):

$$I = \frac{1}{2} \cdot \sum_i z_i^2 [X]_i \qquad [8]$$

The tabulated constants in Martell & Smith (19, 20) were corrected to the calculated ionic strength using the equations in Harrison & Bers (11). The calculated values for K_{app} as well as the measured K_{app} values are summarised in table 2. K_{app} values were calculated for the minimum and maximum of the calculated pH_c values. However, the K_{app} values for malate and citrate showed little pH_c dependence over the pH_c range 7.0 to 7.5. This was not the case for aspartate, but in all cases the mean values of the K_{app} at the two pH_c values were used to calculate the $[Mg^{2+}]_o$ and $[Ca^{2+}]_o$.

A comparison between calculated and measured $[Mg^{2+}]_o$ in the presence of aspartate, malate and citrate, and $[Ca^{2+}]_o$ in the presence of malate is illustrated in figure 8. For aspartate and Mg^{2+}, the calculated K_{app} at an ionic strength of 0.1 mol/l is some 8 times greater than that measured. Even after correction for ionic strength there is no agreement between calculated and measured concentrations as illustrated in figure 8A. For Mg^{2+} with malate or citrate there is limited agreement (figure 8B and 8C); this is also true for Ca^{2+} and malate (figure 8D). In these latter cases, the measured ionic concentrations are less than the calculated concentrations in all cases. If the ionic strength were less, the agreement would be better; therefore, the question arises whether using equation [8]

Table 2. Comparison between measured and calculated K_{app} values

Solutions	Ionic Strength	K_{app}-Measured	K_{app}-Calculated		
	(mol/l)	mean±SD (mmol/l)	pH_{min} (mmol/l)	pH_{max} (mmol/l)	Mean (mmol/l)
Magnesium					
Aspartate-Na^+	0.1140	101.7±22.5 (n = 8)	833.54	865.07	849.30
Aspartate-K^+	0.1532		894.09	942.93	918.51
Constants	0.1000		808.74	833.98	821.36
Ionic equivalent	0.1040		811.25	834.07	822.66
Malate-Na^+	0.1040	15.85±1.01 (n = 7)	20.52	20.52	20.52
Malate-K^+	0.1532		26.68	26.68	26.68
Constants	0.1000		20.00	20.00	20.00
Ionic equivalent	0.0940		19.19	19.19	19.19
Citrate-Na^+	0.1140	0.332±0.136 (n = 4)	0.498	0.498	0.498
Constants	0.1000		0.437	0.437	0.437
Ionic equivalent	0.0890		0.389	0.389	0.389
Calcium					
Malate-Na^+	0.1240	10.32±1.07 (n = 7)	12.70	12.70	12.70
Constants	0.10000		10.99	10.99	10.99
Ionic equivalent	0.0940		10.55	10.55	10.55

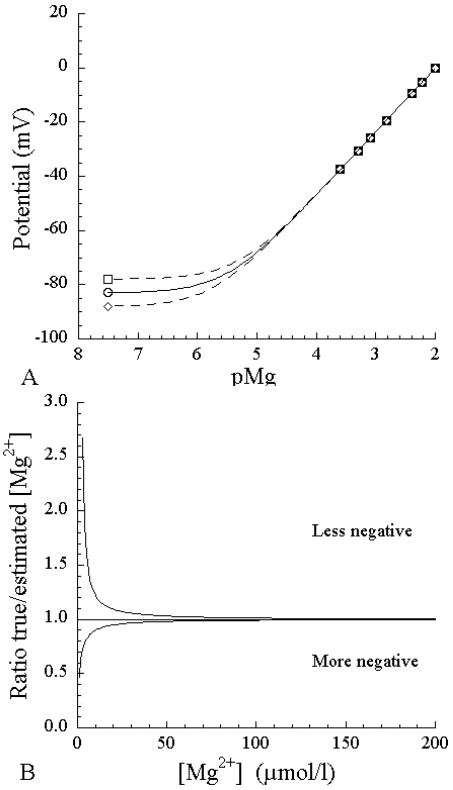

Figure 7. Influence of deviations of the measured potential in the ligand solutions on the calculated concentrations. **A.** Solid line, mean calibration curve for Mg^{2+} macroelectrodes (see Figure 2). The dashed lines represent the ± 5 mV from the mean value at pMg of 7.5 (-82.89 mV). Curves have been fitted by the Nicolsky-Eisenman equation: +5 mV (upper curve): Potential = 47.1006 + 23.5503*log(10^{-pMg} + 4.89*10^{-6}); r = 0.99999987 -5 mV (lower curve): Potential = 46.9910 + 23.4955*log(10^{-pMg} +1.78*10^{-6}); r = 0.99999996. **B.** Ratio of the true/estimated concentrations over the range 1 µmol/l to 200 µmol/l. At concentrations greater than 50 µmol/l, even with deviations as large as ± 5 mV the ratio approaches the value of one.

is the appropriate method to estimate the effects of ionic interaction. Johansson (16) introduced the concept of ionic equivalents, defined as follows:

$$I = \frac{1}{2} \cdot \sum_i z_i [X]_i \qquad [9]$$

Smith & Miller (29) found that using this concept there was a better fit between calculated and measured results for the Ca^{2+} binding constant of EGTA. The ionic equivalents of the solutions are shown in table 1 and the calculated K_{app} using this formulation are shown in table 2. For aspartate, using the ionic equivalent made no difference. There was a slight reduction in the K_{app} for Mg^{2+} binding to malate that was insufficient to improve the fit. As shown in figure 8C and 8D, using the ionic equivalent did improve the fit for Mg^{2+} binding to citrate and for the binding of Ca^{2+} to malate.

In conclusion, there was no agreement between measured and calculated $[Mg^{2+}]_o$ for aspartate. The agreement between calculated and measured free $[Mg^{2+}]_o$ in the presence of malate and citrate was limited, even if ionic equivalents are used instead of ionic strength. In contrast, the use of ionic equivalents to calculate free $[Ca^{2+}]_o$ gave excellent agreement between measured and calculated free concentrations. Measurement of Mg^{2+} binding to citrate indicated a di-Mg-citrate complex with a low affinity, which would not have been predicted from the constants in Martell & Smith (20). There are again the problems of converting pH_a to pH_c (see table 1). The measurements made in this paper were carried out at room temperature around 22°C. The tabulated constants in Martell & Smith (19, 20) for aspartate are for 20°C and 25°C, those for citrate and malate only for 25°C. While the enthalpy values for the protonation constants are tabulated, none are available for the Mg^{2+} and Ca^{2+} constants. Thus it is not possible to estimate K_{app} at other temperatures. With these considerations in mind and given the relative ease of measurement, measurement of the free concentrations in biological solutions at the appropriate ionic strength and temperature would seem prudent rather than relying on calculations and its many underlying assumptions.

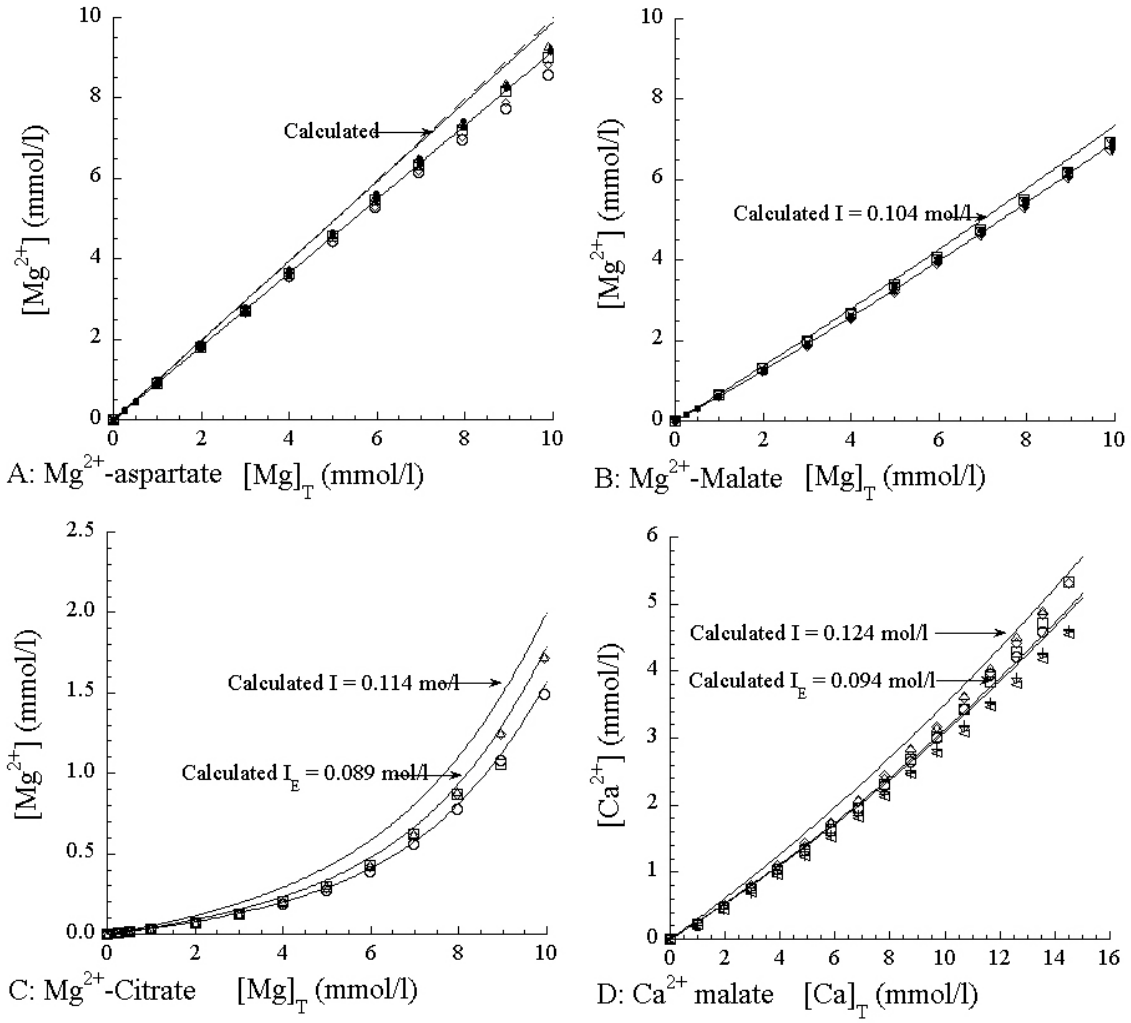

Figure 8. Comparison between measured and calculated concentrations. All plots are shown as $[Mg]_T$ against $[Mg^{2+}]$ calculated as in Figures 3 to 6. The Figures all show the fit calculated from the mean measured K_{app}. The values of the appropriate K_{app} are taken from table 2. **A.** Mg^{2+}-aspartate. In this plot, the dashed line represents the line of equality between $[Mg]_T$ and $[Mg^{2+}]$ *i.e.,* no binding. The continuous line just under the dashed line is calculated using the mean value of the K_{app} calculated for an ionic strength of 0.1 mol/l. Although not shown, there was little difference in the calculated curves for ionic strength of 0.114 mol/l and 0.15325 mmol/l. **B.** Mg^{2+}-malate. This shows the calculated curves for ionic strengths of 0.104 mol/l. Using the ionic equivalent gave a very similar calculated curve. For clarity it is not shown. **C**. To simplify the fit only one binding site has been assumed. This shows both the ionic strength of 0.114 mmol/l and the ionic equivalent (I_E) of 0.089 mol/l. **D**. Ca^{2+} binding to malate. The plot shows the values for ionic strength of 0.124 mol/l and the ionic equivalent (I_E) of 0.094 mol/l.

5.3.2. Biological relevance of the binding

Experimentally it has been found that an infusion of $MgSO_4$ reduced infarct size; in contrast, Grunert *et al.* (7) found that an infusion of Mg aspartate did not. One possibility to explain this disagreement is that Mg^{2+} binding to aspartate might have resulted in a lower free serum $[Mg^{2+}]_o$ compared to that obtained through use of $MgSO_4$. In the experiments of Grunert *et al.* $[Mg]_T$ increased from a mean value of 0.65 mmol/l to just under 2 mmol/l. While it is not possible to calculate the $[Mg^{2+}]_o$ changes during the experiment exactly, the measured K_{app} of 45.2 mmol/l suggests that using aspartate instead of sulphate, $[Mg^{2+}]_o$ would be reduced by about 5% at a $[Mg]_T$ of 2 mmol/l. This seems far too small a difference to account for the contrasting results. The temperature of these measurements varied by ± 5°C around 39°C, the body temperature of the dog. However, even if the K_{app} was 25 mmol/l the reduction in the free Mg^{2+} concentration would only be some 12%. While such results do not support a decrease in the free $[Mg^{2+}]_o$ as the cause of the difference between the results with aspartate and sulphate it would appear essential in future experiments with aspartate, to actually measure the free $[Mg^{2+}]_o$ in plasma during the experiment (7).

Instead, perhaps aspartate could be acting as a glutamate receptor agonist. It has recently been shown that heart possesses both ionotropic and metabolic glutamate receptors so a direct action of aspartate on heart is a distinct possibility (see Discussion in 25). A direct comparison between the effects of Mg-di-aspartate and $MgSO_4$ on

infarct size in an animal model would now seem to be appropriate.

As mentioned above, binding between Mg^{2+} and organic anions is of biological importance in the medicinal leech (*Hirudo medicinalis*). In the leech, Cl^- accounts only for about 30% of the extracellular anions, while the remainder is made up of organic anions. Under physiological conditions the most prevalent of these is malate, with concentrations up to 30 mmol/l (13). $[Mg^{2+}]_T$ in leech blood as determined by atomic absorption spectrometry has a mean ± SD of 1.64 ± 0.52 mmol/l (n = 3, unpublished results). At an extracellular malate concentration of 30 mmol/l and a K_{app} of 15.5 mmol/l, as determined in the present study, this corresponds to a $[Mg^{2+}]_o$ of 0.57 ± 0.18 mmol/l, which is in excellent agreement with the $[Mg^{2+}]_o$ of 0.6 ± 0.2 mmol/l determined by Hildebrandt & Zerbst-Boroffka (12). $[Mg^{2+}]_o$ in the leech is thus strongly buffered. This may be of vital importance to the leech as total ion concentrations change considerably during feeding (32). Changes in $[Mg^{2+}]_o$ are known to affect neuronal transmission, and it has recently been demonstrated that changes in $[Mg^{2+}]_o$ influence the properties of the neuronal network creating the heart rhythm in the leech (31). Furthermore, in neurones from the central nervous system of the leech, malate and Mg^{2+} appear to be co-transported across the cell membrane (9). While under experimental conditions in Cl^--based bath solutions this is an outward transport, under physiological conditions it has been postulated that this mechanism mediates an uptake of malate from the blood into neurones. Investigations of the substrate specificity of this transport mechanism demonstrated that the most potent activators of this transport were malate and citrate. As both anions bind Mg^{2+}, this transport may be able to significantly alter the intracellular Mg^{2+}-buffering capacity.

5.4. Summary

Using Mg^{2+} and Ca^{2+} macroelectrodes as described in this report, it is possible to accurately measure ionised concentrations of these cation down to a lower limit of about 50 µmol/l without the use of Mg^{2+} and Ca^{2+} buffer solutions. Calculation of ionised concentrations using tabulated constants cannot be recommended for biological solutions, as even for malate and citrate there was only approximate agreement between calculated and measured concentrations. *Measurement*, although time consuming, is much more accurate.

6. ACKNOWLEDGEMENTS

We would like to thank Dr. Federica Wolf (Rome) for carrying out the AAS measurements. JMcG would like to thank DG and WRS for their hospitality during his stay in Düsseldorf. Supported by the DFG (Gu447/6-1).

7. REFERENCES

1. Atkins, P. W.: Physical Chemistry, 4th Edition. Oxford University Press. Oxford, UK (1990)
2. Bates, R. G.: Determination of pH. Theory and Practice. Wiley, New York, NY (1973)
3. Burton, R. F.: Ringer Solutions and Physiological Salines. Wright Scientechnica, Bristol, UK (1975)
4. Classen, H. G.: Magnesium-L-aspartate hydrochloride: experimental and clinical data. *J Clin Basic Cardiol*, 5, 43-47 (2002)
5. Davies, C. W.: Electrochemistry. George Newnes Ltd., London, UK (1967)
6. Fry, C. H. & C. E. M. Langley: Ion–selective Electrodes for Biological Systems. Harwood Academic Publishers, Reading, UK (2000)
7. Grunert, S., D. Ebel, W. Schlack & V. Thämer: Intracoronary and intravenous magnesium does not reduce myocardial infarct size in a canine model of regional ischaemia and reperfusion. *J Clin Basic Cardiol*, 5, 23-28 (2002)
8. Günzel, D. & W.-R. Schlue: Determination of $[Mg^{2+}]_i$ - an update on the use of Mg^{2+}-selective electrodes. *Biometals*, 15, 237-249 (2002)
9. Günzel, D., K. Hintz, S. Durry & W.-R. Schlue: Organic anion-dependent Mg^{2+} extrusion from leech neurones. *Pflügers Arch*, 443, S240 (2002)
10. Hamer, W. J. & Y. C. Wu: Osmotic coefficients and mean activity coefficients of uni-valent electrolytes in water at 25°C. *J Phys Chem Ref Data*, 4, 1047-1099 (1972)
11. Harrison, S. M. & D. M. Bers: Correction of proton and Ca association constants of EGTA for temperature and ionic strength. *Am J Physiol*, 256, C1250-C1256 (1989)
12. Hildebrandt, J. P. & I. Zerbst-Boroffka: Osmotic and ionic regulation during hypoxia in the medicinal leech, *Hirudo medicinalis*. *J Exp Zool*, 263, 374-381 (1992)
13. Hoeger, U., A. Wenning & U. Greisinger: Ion Homeostasis in the leech: contribution of organic anions. *J Exp Biol*, 147, 43-51 (1989)
14. Huijgen, H. J., H. E. van Ingen, W. Th. Kok & G. T. B. Sanders: Magnesium fractions in serum of healthy individuals and CAPD patients, measured by an ion-selective electrode and ultrafiltration. *Clin Biochem*, 29, 261-266 (1996)
15. Huijgen, H. J., R. Sanders, S. A. Cecco, N. N. Rehak, G. T. Sanders & R. J. Elin: *Clin Chem Lab Med*, 37, 465-470 (1999)
16. Johansson, L.: Some aspects of the constant ionic medium principle. Studies on iron III fluoride and tris (propylenediamine) cobalt III iodide systems. *Acta Chem Scand A*, 29, 365-373 (1975)
17. Lüthi, D., U. Spichiger, I. Forster & J.A.S. McGuigan: Calibration of Mg^{2+}-selective macroelectrodes down to 1 $\mu moll^{-1}$ in intracellular and Ca^{2+}-containing extracellular solutions. *Exp Physiol*, 82, 453-467 (1997)
18. Lüthi, D., D. Günzel & J. A. S. McGuigan: Mg-ATP binding: its modification by spermine, the relevance to cytosolic Mg^{2+} buffering, changes in the intracellular ionised Mg^{2+} concentration and the estimation of Mg^{2+} by ^{31}P-NMR. *Exp Physiol*, 84, 231-252 (1999)
19. Martell, A. E. & R. M. Smith: Critical Stability Constants: Volume 1, Amino Acids. Plenum Press, New York, NY (1974)
20. Martell, A. E. & R. M. Smith: Critical Stability Constants: Volume 3, Other Organic Ligands. Plenum Press, New York, NY (1977)

21. McGuigan, J. A. S., D. Lüthi & A. Buri: Calcium buffer solutions and how to make them: a do-it yourself guide. *Can J Physiol Pharmacol*, 69, 1733-1749 (1991)
22. McGuigan, J. A. S., A. Buri, S. Chen, H. Illner & D. Lüthi: Some theoretical and practical aspects of the measurement of the intracellular free magnesium concentration in heart muscle: consideration of its regulation and modulation. In: Magnesium and the cell. Ed: Birch, N. J., pp 91-120, Academic Press, London, UK (1993)
23. McGuigan, J. A. S., T. Günther, D. Lüthi, H. Elder & A. Johnson: Advantages and pitfalls when using Mg^{2+} macroelectrodes to measure the free Mg^{2+} concentration in cell or membrane vesicle suspensions, or in Mg^{2+}-ligand binding studies. *Magnesium-Bull*, 19, 110-118 (1997)
24. McGuigan, J. A. S., H. Y. Elder, D. Günzel & W.-R. Schlue: Magnesium homeostasis in heart: a critical reappraisal. *J Clin Basic Cardiol*, 5, 5-22 (2002)
25. Müller, A., D. Günzel & W.-R. Schlue: Activation of AMPA kainate receptors but not acetylcholine receptors causes Mg^{2+} influx into Retzius neurones of the Leech *Hirudo medicinalis*. *J Gen Physiol*, 122, 727-739 (2003)
26. O'Donell, J., H. Li, B. Rusterholz, U. Pedrazza & W. Simon: Development of magnesium-selective ionophores. *Anal Chim Acta*, 281, 129-134 (1993)
27. Oehme, M., M. Kessler & W. Simon: Neutral carrier Ca^{2+}-microelectrode. *Chim*, 30, 204-206 (1976)
28. Saris, N.-E. L., E. Mervaala, H. Karppanen, J. A. Khawaja & A. Lewenstam: *Clin Chim Acta*, 294, 1-26 (2000)
29. Smith, G. L. & D. J. Miller: Potentiometric measurements of stoichiometric and apparent affinity constants of EGTA for protons and divalent ions including calcium. *Biochim Biophys Acta*, 839, 287-299 (1985)
30. Spätling, L., H. G. Classen, W. R. Külpmann, F. Manz, P. M. Rob, H. F. Schimatschek, W. Vierling, J. Vormann, A. Weigert & K. Wink: Diagnostik des Magnesiummangels. Aktuelle Empfehlungen der Gesellschaft für Magnesium-Forschung e.V. *Fortschr Med*, 118, 49-53 (2000)
31. Weinhold, H., D. Günzel & W.-R. Schlue: Extracellular Mg^{2+} modulates the neuronal network controlling the heartbeat of the leech. *Trace Elem Electrolytes*, 20, 201 (2003)
32. Wenning, A., I. Zerbst-Boroffka & B. Bazin: Water and salt excretion in the leech (*Hirudo medicinalis*). *J Comp Physiol* 139, 97-102 (1980)
33. Westergaard, N., U. Sonnewald, G. Unsgård, L. Peng, L. Hertz & A. Schousboe: Uptake, release, and metabolism of citrate in neurons and astrocytes in primary culture. *J. Neurochem*. 62, 1727-1733 (1994)
34. Zhang, W., A. C. Truttmann, D. Lüthi & J. A. S. McGuigan: The manufacture and characteristics of magnesium selective macroelectrodes. *Magnesium-Bull*, 17, 125-130 (1995)
35. Zhang, W., A. C. Truttmann, D. Lüthi & J. A. S. McGuigan: Apparent Mg^{2+}-adenosine 5-triphosphate dissociation constant measured with Mg^{2+} macroelectrodes under conditions pertinent to ^{31}P NMR ionised magnesium determinations. *Anal Biochem*, 251, 246-250 (1997)
36. Zhang, X., A. Fakler & U. E. Spichiger: Development of magnesium-ion-selective microelectrodes based on a new neutral carrier ETH 5504. *Electroanal,* 10, 1174-1181 (1998)

8. APPENDIX

8.1. Definitions

Drift:

E_1, E_2, ...E_n	Potentials in solutions 1, 2, ...n; mV
A	Constant of the recording system; mV
s	Electrode slope; mV/decade
ΔE	Drift of the macroelectrode over a given time interval; mV
$\Delta[X^{2+}]$	Apparent change in concentration calculated from drift ; mmol/l

Binding:

$[X^{2+}]_1$, $[X^{2+}]_2$...$[X^{2+}]_n$	Concentrations of free Mg^{2+} and Ca^{2+} in solutions 1, 2, n, ; mmol/l
$[X]_T$	Total concentration of Mg^{2+} and Ca^{2+} ; mmol/l
$[Anion^{n-}]$	Concentration of free anion; mmol/l
$[X\text{-}Anion^{(n-2)-}]$	Concentration of anion binding 1 X^{2+}; mmol/l
$[X_2\text{-}Anion^{(n-4)-}]$	Concentration of anion binding 2 X^{2+}; mmol/l
$[X\text{-}Anion]_B$	Concentration of bound Mg^{2+} and Ca^{2+} equal to ($[X]_T$ - $[X^{2+}]$); mmol/l
$[Anion]_T$	Total concentration of anion; mmol/l
K_{app}	Apparent equilibrium constant; mmol/l
K_2	Second citrate equilibrium constant for Mg^{2+}; mmol/l

8.2. Apparent concentration changes due to drift

Drift can be regarded as a change in concentration. The potentials at two different concentrations are:

$$E_1 = A + s\log\left(\frac{[X^{2+}]_1}{1000}\right) \text{ and } E_2 = A + s\log\left(\frac{[X^{2+}]_2}{1000}\right) \quad [1][2]$$

The difference in potential between the two solutions is:

$$\Delta E = s\log\left(\frac{[X^{2+}]_1}{1000}\right) - s\log\left(\frac{[X^{2+}]_2}{1000}\right) \quad [3]$$

or

$$\Delta E = s\log\left(\frac{[X^{2+}]_1}{[X^{2+}]_2}\right) \quad [4]$$

From equation [4], the ratio of the concentrations is:

$$\left(\frac{[X^{2+}]_1}{[X^{2+}]_2}\right) = 10^{\frac{\Delta E}{s}} \quad [5]$$

If drift is negative, $[X^{2+}]_2 = [X^{2+}]_1 \cdot 10^{\frac{-\Delta E}{s}}$ [6]

if positive, $[X^{2+}]_2 = [X^{2+}]_1 \cdot 10^{\frac{+\Delta E}{s}}$ [7]

The apparent change in concentration from $[X^{2+}]_1$ to $[X^{2+}]_2$ is:

$$\Delta[X^{2+}] = [X^{2+}]_1 \cdot \left(10^{\frac{\pm\Delta E}{s}} - 1\right) \quad [8]$$

8.3. Cation binding to anions

8.3.1. Binding of one cation

$$\left[X^{2+}\right]+\left[Anion^{n-}\right]\leftrightarrow\left[X-Anion^{(n-2)-}\right] \quad [9]$$

At equilibrium:

$$K_{app}=\frac{\left[X^{2+}\right]\left[Anion^{n-}\right]}{\left[X-Anion^{(n-2)-}\right]} \quad [10]$$

Total concentrations of X^{2+} and $Anion^{n-}$ are:

$$[X]_T=\left[X^{2+}\right]+\left[X-Anion^{(n-2)-}\right] \quad [11]$$

and

$$[Anion]_T=\left[Anion^{n-}\right]+\left[X-Anion^{(n-2)-}\right] \quad [12]$$

$[X\text{-}Anion^{(n-2)-}]$:

Substituting for $[Anion^{n-}]$ from equation [12] in equation [10] gives:

$$K_{app}=\frac{\left[X^{2+}\right]\left([Anion]_T-\left[X-Anion^{(n-2)-}\right]\right)}{\left[X-Anion^{(n-2)-}\right]} \quad [13]$$

Rearranging and solving for $[X\text{-}Anion^{(n-2)-}]$:

$$\left[X-Anion^{(n-2)-}\right]=\frac{\left[X^{2+}\right][Anion]_T}{\left(K_{app}+\left[X^{2+}\right]\right)} \quad [14]$$

$[X^{2+}]$:

Substitution for $[X\text{-}Anion^{(n-2)-}]$ from equation [11] in equation [13] gives:

$$K_{app}=\frac{\left[X^{2+}\right]\left\{[Anion]_T-\left([X]_T-\left[X^{2+}\right]\right)\right\}}{\left([X]_T-\left[X^{2+}\right]\right)} \quad [15]$$

Simplification gives:

$$\left[X^{2+}\right]^2+\left([Anion]_T+K_{app}-[X]_T\right)\left[X^{2+}\right]-K_{app}[X]_T=0 \quad [16]$$

The solution of the quadratic is:

$$\left[X^{2+}\right]=\frac{-\left([Anion]_T+K_{app}-[X]_T\right)+\sqrt{\left([Anion]_T+K_{app}-[X]_T\right)^2+4K_{app}[X]_T}}{2} \quad [17]$$

8.3.2. Binding of two cations

$$\left[X^{2+}\right]+\left[Anion^{n-}\right]\leftrightarrow\left[X-Anion^{(n-2)-}\right] \quad [18]$$

and

$$\left[X^{2+}\right]+\left[X-Anion^{(n-2)-}\right]\leftrightarrow\left[X_2-Anion^{(n-4)-}\right] \quad [19]$$

At equilibrium

$$K_{app}=\frac{\left[X^{2+}\right]\left[Anion^{n-}\right]}{\left[X-Anion^{(n-2)-}\right]} \quad [20]$$

and

$$K_2=\frac{\left[X^{2+}\right]\left[X-Anion^{(n-2)-}\right]}{\left[X_2-Anion^{(n-4)-}\right]} \quad [21]$$

The total concentrations are:

$$[X]_T=\left[X^{2+}\right]+\left[X-Anion^{(n-2)-}\right]+2\left[X_2-Anion^{(n-4)-}\right] \quad [22]$$

and

$$[Anion]_T=\left[Anion^{n-}\right]+\left[X-Anion^{(n-2)-}\right]+\left[X_2-Anion^{(n-4)-}\right] \quad [23]$$

The concentration of bound X^{2+} is:

$$[X-Anion]_B=\left([X]_T-\left[X^{2+}\right]\right) \quad [24]$$

Substituting for $\left([X]_T-\left[X^{2+}\right]\right)$ from equation [22] in equation [24] gives:

$$[X-Anion]_B=\left[X-Anion^{(n-2)-}\right]+2\left[X_2-Anion^{(n-4)-}\right] \quad [25]$$

Substitution of equations [20] and [21] in equation [25]:gives:

$$[X-Anion]_B=\frac{\left[X^{2+}\right]\left[Anion^{n-}\right]}{K_{app}}+\frac{2\left[X^{2+}\right]^2\left[Anion^{n-}\right]}{K_{app}K_2} \quad [26]$$

$[Anion^{n-}]$ in terms of K_{app}, K_2 and $[Anion]_T$:

From equation [23]:

$$\left[Anion^{n-}\right]=[Anion]_T-\left[X-Anion^{(n-2)-}\right]-\left[X_2-Anion^{(n-4)-}\right] \quad [27]$$

Substitution of equations [20] and [21] in equation [27]

$$\left[Anion^{n-}\right]=[Anion]_T-\frac{\left[X^{2+}\right]\left[Anion^{n-}\right]}{K_{app}}-\frac{\left[X^{2+}\right]^2\left[Anion^{n-}\right]}{K_{app}K_2} \quad [28]$$

and

$$\left[Anion^{n-}\right]=\frac{[Anion]_T}{\left(1+\frac{\left[X^{2+}\right]}{K_{app}}+\frac{\left[X^{2+}\right]^2}{K_{app}K_2}\right)} \quad [29]$$

Substitution of equation [29] in equation [26] gives:

$$[X-Anion]_B=\frac{\left[X^{2+}\right][Anion]_T}{\left(K_{app}+\left[X^{2+}\right]+\frac{\left[X^{2+}\right]^2}{K_2}\right)}+\frac{2\left[X^{2+}\right]^2[Anion]_T}{K_2\left(K_{app}+\left[X^{2+}\right]+\frac{\left[X^{2+}\right]^2}{K_2}\right)} \quad [30]$$

$[X^{2+}]$:

Substituting equations [20] and [21] in equation [22]:

$$[X]_T=\left[X^{2+}\right]+\frac{\left[X^{2+}\right]\left[Anion^{n-}\right]}{K_{app}}+\frac{2\left[X^{2+}\right]^2\left[Anion^{n-}\right]}{K_{app}K_2} \quad [31]$$

Substituting equation [29] in equation [31]

$$[X]_T=\left[X^{2+}\right]+\frac{\left[X^{2+}\right][Anion]_T}{K_{app}\left(1+\frac{\left[X^{2+}\right]}{K_{app}}+\frac{\left[X^{2+}\right]^2}{K_{app}K_2}\right)}+\frac{2\left[X^{2+}\right]^2[Anion]_T}{K_{app}K_2\left(1+\frac{\left[X^{2+}\right]}{K_{app}}+\frac{\left[X^{2+}\right]^2}{K_{app}K_2}\right)} \quad [32]$$

or

$$\begin{aligned}&[X]_TK_{app}K_2\left(1+\frac{\left[X^{2+}\right]}{K_{app}}+\frac{\left[X^{2+}\right]^2}{K_{app}K_2}\right)=\\&=\left[X^{2+}\right]K_{app}K_2\left(1+\frac{\left[X^{2+}\right]}{K_{app}}+\frac{\left[X^{2+}\right]^2}{K_{app}K_2}\right)+\\&+K_2\left[X^{2+}\right][Anion]_T+2\left[X^{2+}\right]^2[Anion]_T\end{aligned} \quad [33]$$

Simplification gives:

$$\begin{aligned}&\left[X^{2+}\right]^3+\left(K_2+2[Anion]_T-[X]_T\right)\left[X^{2+}\right]^2+\\&+K_2\left(K_{app}+[Anion]_T-[X]_T\right)\left[X^{2+}\right]-[X]_TK_{app}K_2=0\end{aligned} \quad [34]$$

Key Words: Macroelectrodes, Mg^{2+} and Ca^{2+} Binding, Organic Anions, Mg^{2+}, Ca^{2+}, Buffering

Send correspondence to: John A. S. McGuigan, Walchstrasse 12, 3073 Gümligen, Switzerland, Tel and Fax: +41-31-951 2162, E-mail: jasmcguigan@yahoo.com

http://www.bioscience.org/current/vol10.htm